



Synthesis of efficient activated carbon from *Peltophorum pterocarpum* for the adsorption of Safranin O and its investigation on equilibrium, kinetic, and thermodynamic studies

Y. Subbareddy, C. Jayakumar, S. Valliammai, K.S. Nagaraja, B. Jeyaraj*

Department of Chemistry, Loyola Institute of Frontier Energy (LIFE), Loyola College, Chennai, Tamil Nadu 600034, India, Fax: +91 44 28175566; email: jeyaraj.boniface@gmail.com (B. Jeyaraj)

Received 10 March 2014; Accepted 28 April 2014

ABSTRACT

Activated carbon with efficient adsorption capacity was prepared using *Peltophorum pterocarpum* leaves impregnated with phosphoric acid. The prepared activated carbon (PAC) was characterized for their surface functional groups by Fourier transform infrared spectroscopy and for their surface morphology and chemical composition by Scanning Electron Microscopy with Energy Dispersive X-ray analysis. X-ray diffraction and Raman studies revealed that the graphitic and nanocrystalline nature of PAC. The surface area ($409.01 \text{ m}^2/\text{g}$) of the PAC was determined by Brunauer Emmet and Teller method and the material was found to be mesoporous. The thermal stability of PAC was studied with thermogravimetric analysis. The effects of contact time, adsorbent dose, initial dye concentration at different temperatures and pH on the removal percentage of Safranin O (SO) dye were investigated. With increase in contact time, adsorbent dose, pH, and temperature, an increase in the removal of SO dye was observed. The experimental data were examined using Langmuir, Freundlich, and Dubinin–Radushkevich adsorption isotherms. The Langmuir model gave the best fit for the uptake of SO dye confirming that the adsorption of SO dye onto PAC was homogeneous in nature with mono layer adsorption capacity of $6.325 \times 10^{-4} \text{ mol/g}$. Pseudo-first-order and pseudo-second-order models were used to determine the adsorption kinetics and it was observed that the adsorption of SO dye followed the pseudo-second-order model ($R^2 = 0.999$). Thermodynamic parameters ΔG° , ΔH° , and ΔS° were evaluated to determine the spontaneity and endothermic nature of the adsorption process.

Keywords: *Peltophorum pterocarpum*; Safranin O; Activated carbon; Kinetics; Isotherms

1. Introduction

In recent years, the depletion of natural resources like water on the planet earth has become rapid. This is mainly due to water pollution which is arising from the industries such as textile, paper, rubber, plastic,

leather, cosmetic, etc. Invariably these industries use the dyes and pigments in large quantities to color their products [1]. The disposal of colored wastes into water streams is very dangerous, as they are toxic and carcinogenic and also not biodegradable [2]. They pose danger to the flora and fauna in the biosphere, therefore it is mandatory to remove these compounds from the wastewater before their safe disposal into the

*Corresponding author.

surface waters. To remediate against such environmental hazards, the various treatment technologies like physical and chemical methods have been used for the treatment of industrial wastewaters. These methods include ozonation [1], coagulation [3], precipitation [3], reverse osmosis [4], photo degradation [5], electrochemical oxidation [6], and adsorption [7,8].

Adsorption process is considered to be one of the most efficient, economic, and versatile technique, in removing the pollutants from wastewater without leaving any toxic by-products [8]. Adsorption has been found to be more promising than the other techniques in terms of cost effectiveness, simplicity of design, and ease of implementation. A variety of adsorbents such as activated carbon, silica, alumina, bentonite, chitosan [9,10], and ion-exchange resins have been used for the removal of colored organics from aqueous solutions. Among these, activated carbon is one of the most widely used adsorbent for the removal of colored organics, but it is costly and cannot be recycled so easily. Hence, there is a great need to develop alternative adsorbents, preferably low-cost adsorbents which do not require expensive setup. Many researchers have been working in this direction for the removal of toxic dyes from the wastewater using low-cost adsorbents like, bottom ash [11], de-oiled soya [12], hen feathers [13–18], coal, lignite, coconut shells, wood, and peat [19,20].

The aim of this work is to test the adsorption behavior of the activated carbon prepared from the leaves of *Peltophorum pterocarpum* for the removal of toxic dye Safranin O (SO) and it is novel idea for the water treatment process. SO is an organic dye, belonging to the quinone–imine class, and is widely used for counterstaining purposes [21]. It also used in textile, leather, and paper industries. Since the dye is known to be carcinogenic in nature, small amount of this dye in wastewater would have detrimental effects on aquatic environment [21]. The effect of various parameters such as contact time, adsorbent dose, initial dye concentration, temperature, and pH for the removal of SO dye is studied. Equilibrium, kinetic, and thermodynamic parameters are also investigated.

2. Materials and methods

2.1. Preparation of activated carbon

P. pterocarpum is a moderate sized, well-shaped evergreen tree with a dense crown [22]. It is native to South India and Tropical South East Asia. This tree is widely grown in tropical regions as an ornamental tree and grows rapidly. *P. pterocarpum* leaves were dried at room temperature. After grinding to a fine

powder, the mass was oven dried at 110°C for 2 h. The dried mass was impregnated with H₃PO₄ (85 wt.%) in the ratio of 5:1 (g H₃PO₄/g *P. pterocarpum* leaves powder) and allowed to carbonize at 450°C in a muffle furnace for 1 h. The obtained carbon material was washed with distilled water until a constant pH of the solution reached and dried overnight at 110°C.

2.2. Description of adsorbate SO

SO dye is a cationic dye (Fig. 1) having the IUPAC name as 3,7-diamino-2,8-dimethyl-5-phenyl-phenazinium chloride. The stock solution of the dye was prepared in double distilled water. All the test solutions were prepared by diluting the stock solution with double distilled water. The λ_{\max} of SO is 520 nm.

2.3. Characterization

The Fourier transform infrared spectroscopy (FTIR) spectrum was recorded using Thermo Nicolet, Avatar 370 FTIR spectrophotometer. FEI Quanta FEG 200 High Resolution instrument was used for Scanning Electron Microscopy (SEM) images. X-ray diffraction (XRD) pattern was recorded from 10 to 80° with Cu K α as the X-ray source ($\lambda = 1.54 \text{ \AA}$) using Bruker's AXS Model D8 Advance System. Raman spectroscopic study was carried out using Lab Ram HR800 Raman spectrometer; 532 nm green line of Ar⁺ ion laser was used as the excitation source. Brunauer Emmet and Teller (BET) surface area of prepared activated carbon (PAC) was measured by N₂ adsorption/desorption isotherms at 77.18 K using ASAP 2030 Micromeritics instrument. Thermal stability of the activated carbon was studied using EX STAR 6300R TG/DTA with heating rate of 10°C/min in nitrogen atmosphere.

2.4. Adsorption studies

Batch experiments were investigated to study the effect of amount of adsorbent, contact time, the effect

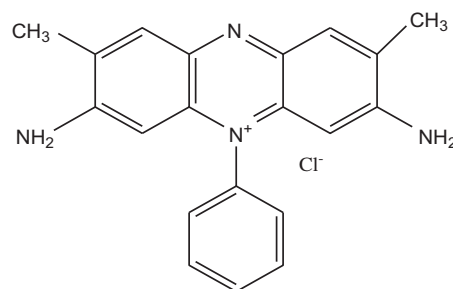


Fig. 1. Chemical structure of SO.

of pH, and initial concentration of the dye at different temperatures on the adsorptive removal of SO. In the adsorption experiments, 50 ml of different concentrations of SO dye solution was taken in each of 100 ml volumetric flask with a known amount of the adsorbent. The flasks were then subjected to mechanical agitation in thermostatic water bath shaker until the equilibrium was reached. These solutions were centrifuged at 5,000 rpm for 15 min and the absorbance of the supernatant solution was measured to determine the residual concentration at λ_{\max} 520 nm using double beam UV Visible spectrophotometer. The remaining dye concentration in aqueous solution was obtained by comparing the absorbance with the calibration curve. The percentage removal and amount adsorbed were calculated from the initial and equilibrium concentration of the dye.

2.5. Adsorption kinetic study

The kinetics of adsorption is an important parameter for determining the efficiency of adsorption and the feasibility of using an adsorbent for wastewater treatment. Hence, the kinetics of removal of the dye has been studied as a function of dye concentration and contact time. For examination of the kinetic and the equilibrium data, a series of 50 ml samples of SO dye of known concentrations (4×10^{-4} M, 5×10^{-4} M, and 6×10^{-4} M) were prepared in airtight 100 ml volumetric flask containing 0.06 g of PAC. The entire sets of flasks with the mixture were mechanically agitated in water bath shaker. The solutions from the flasks were centrifuged at different predetermined intervals of time (5–120 min), and the supernatant solution from each flask was quantified spectrophotometrically. The amount of dye adsorbed (q_t mol/g) at time t was calculated.

3. Results and discussion

3.1. Characterization of PAC adsorbent

3.1.1. Chemical characterization of PAC by Boehm titrations

The Boehm titration method was used to determine the oxygen containing functional groups present over the surface of the activated carbon. 0.5 g of the activated carbon PAC was kept in contact with 50 ml of NaHCO_3 (0.05 N), Na_2CO_3 (0.05 N), and NaOH (0.05 N) for acidic groups and 0.05 N HCl for basic groups, respectively, at room temperature for 24 h. Subsequently, the aqueous solutions were back titrated with HCl (0.05 N) for acidic and NaOH (0.05 N) for basic groups. The difference between the groups titrated

with Na_2CO_3 and those titrated with NaHCO_3 was assumed to be lactone and the difference between the groups titrated with NaOH and those titrated with Na_2CO_3 was assumed to be phenol. Basic sites were determined by titration with HCl . The most common oxygen groups on the surface are carboxylic (0.590 mequiv/g), phenolic (0.51 mequiv/g), lactonic (0.12 mequiv/g), and basic groups (0.181 mequiv/g).

3.1.2. FTIR spectroscopic studies

The broad band around $3,400 \text{ cm}^{-1}$ was observed in all the samples (Fig. 2(a)–(c)), which was attributed to the O–H stretching vibration of hydrogen-bonded hydroxyl groups (from carboxylic, phenolic, or alcoholic) and water adsorbed in the activated carbon. The bands at $2,919.68$ and $2,850.80 \text{ cm}^{-1}$ were due to asymmetric and symmetric C–H stretching vibrations of aliphatic carbon of the raw material (Fig. 2(a)). After carbonization, these vibrations decreased greatly for the activated carbon, indicating that the hydrogen was removed to a large extent [23]. An intense band (Fig. 2(a)) was centered at $1,632 \text{ cm}^{-1}$ which correspond to the carbonyl (C=O) stretching vibration of quinone [24]. The peaks at $1,538$ and $1,453.65 \text{ cm}^{-1}$ indicated the asymmetric and symmetric stretching vibrations of COO^- . The bands around $1,000$ – $1,300 \text{ cm}^{-1}$ are usually found in oxidized carbons and has been assigned to C–O stretching in acids, alcohols, phenols, ethers, and/or ester groups [25]. After the carbonization, all these peaks disappeared, indicating that much of the organic matter was eliminated.

The spectra of the PAC (Fig. 2(b)) showed a strong band at $1,588.73 \text{ cm}^{-1}$ which could be attributed to the carbonyl (C=O) stretching vibration of carboxylic acids, lactones [26]. The band at $1,206.9 \text{ cm}^{-1}$ might be due to C–O stretching frequencies of acids, alcohols, phenols, ethers, and/or ester groups [25]. The FTIR spectrum of activated carbon provided evidence for the presence of surface groups on the adsorbent as determined by Boehm titrations.

After the dye adsorption, the peaks at $3,412.6$, $1,588.73$, and $1,206.9 \text{ cm}^{-1}$ (Fig. 2(c)) were shifted to the wavelengths of $3,413.58$, $1,603.76$, and $1,232.50 \text{ cm}^{-1}$, respectively indicating that OH (from carboxyls, phenols, or alcohols), C=O, and C–O groups of the PAC were involved in the adsorption of SO [27].

3.1.3. XRD spectrum of PAC

The crystallite size of the PAC along c or a directions (L_c or L_a) was determined by [28] Scherrer equation.

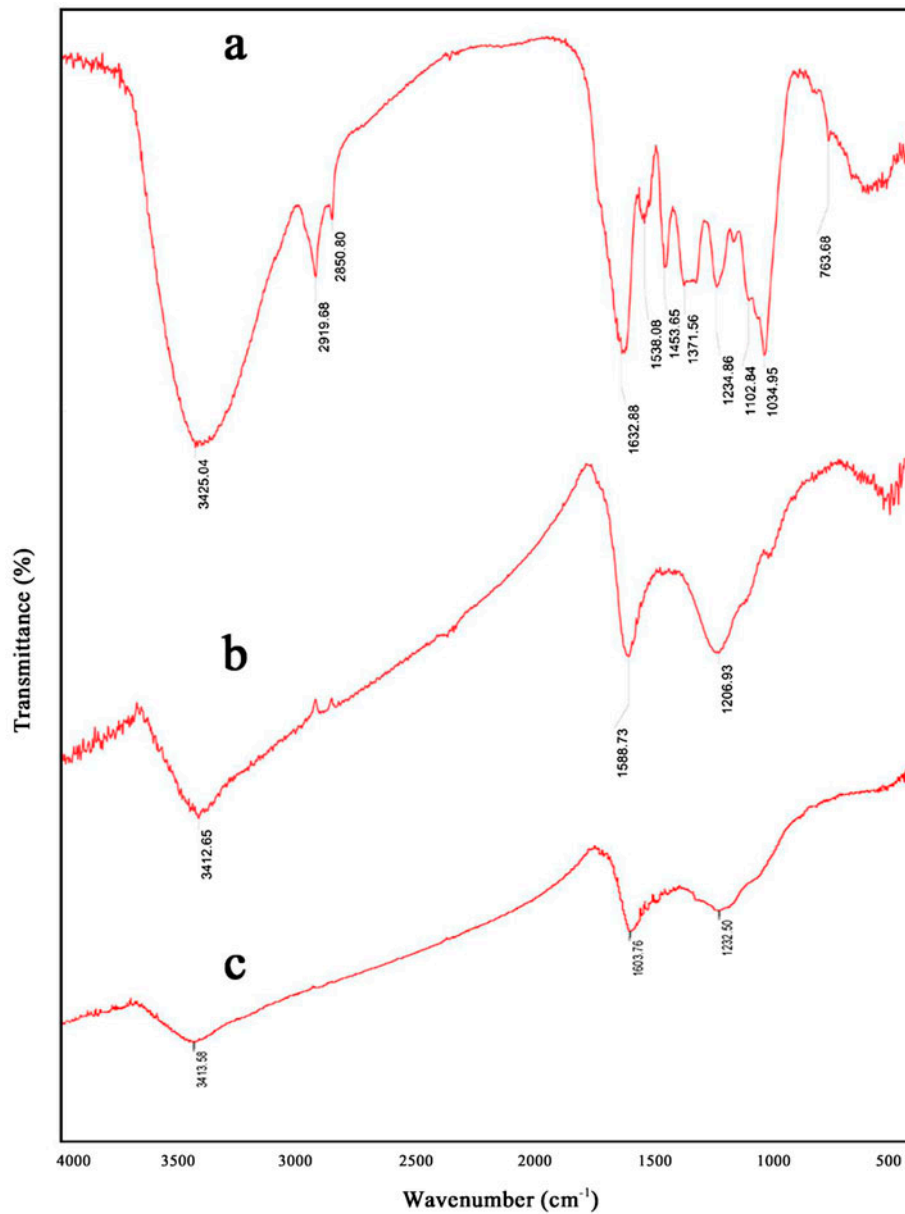


Fig. 2. FTIR spectrum of (a) raw material, (b) activated carbon PAC, and (c) SO adsorbed PAC.

$$L_{c(a)} = \frac{K_{c(a)}\lambda}{\beta_{K_{c(a)}} \cos \theta_{c(a)}} \quad (1)$$

where β is the full width at half maximum of the lines and λ is the X-ray wavelength (0.15406 nm). The shape factor $K_{c(a)}$ is equal to 0.94 and 1.84 for L_c and L_a , respectively. The two diffraction peaks centered at 2θ values of 25.331° and 43.216° were used to calculate L_c (2.709 nm) and L_a (6.655 nm), respectively, which are attributed to 002 and 101 planes of the PAC. The average crystallite size of PAC was found to be 4.682 nm.

The interlayer spacing (d_{002}) was calculated using the Bragg’s law [28]. The value of interlayer distance between two planes was found to be 0.351 nm. The calculated interlayer spacing of PAC was nearer to the standard interlayer spacing of pure graphite carbon [24]. The PAC could be graphitic and nanocrystalline in nature.

3.1.4. Raman spectrum of PAC

The confocal Raman spectrum of PAC material exhibited both the first-order (1,200–1,600 cm^{-1}) and

second-order ($2,400\text{--}3,300\text{ cm}^{-1}$) Raman lines. These Raman lines were used to find out whether it is amorphous or graphitic in nature [24]. The two main peaks of first-order Raman lines were observed in PAC around $1,340\text{ cm}^{-1}$ (D-band) and $1,580\text{ cm}^{-1}$ (G-band), respectively. The D-band was referred as the disorder band, which resulted from the imperfection or loss of hexagonal symmetry of the graphite structure. And the G-band was related to the sp^2 bonded carbon atoms in a two-dimensional hexagonal lattice, which confirmed the formation of ordered graphitic layers [29]. The second-order Raman lines of the recorded spectra showed a broad band around $2,719\text{--}2,955\text{ cm}^{-1}$ which could be attributed to the graphitic carbon. The layers of this graphitic structured carbon in PAC could enhance the adsorption capacity and efficiency.

3.1.5. HR-SEM and EDAX analysis of PAC

The HR-SEM image of PAC before subjecting it to adsorption indicated the presence of various sizes of pores on its surface ranging between 16.4 and 22.3 nm (Fig. 3(a)). It could be inferred that the synthesized activated carbon is nanomaterial in nature. These nanopores were sufficient enough to allow the molecules of the dye to get adsorbed. The chemical composition of PAC was determined using Energy Dispersive X-ray analysis. The EDAX profile showed the presence of carbon (72.37 wt.%) and oxygen (21.81 wt.%) as major constituents of PAC (Fig. 3(b)), as well as small quantities of P and Ca.

3.1.6. BET analysis of PAC

The BET surface area of the PAC was found to be $409.01\text{ m}^2/\text{g}$. The t -plot method was used to determine the micropore volume and mesopore surface area. The mesopore volume was obtained by subtracting the value of micropore volume from the total pore volume. The pore size distribution in the micropore range was obtained using the Horvath–Kawazoe method. PAC exhibited a micropore distribution in the range of 0.7–2.0 nm and indicated that the majority of micropores were supermicropores. The Barret Joyner Halenda pore size distribution indicated that the sample PAC had mesoporosity with pore diameter in the range of 2–5 nm. The average pore diameter of PAC was found to be 4.3 nm which confirms the presence of mesopores. The mesopore and micropore volumes were found to be around 87.32 and 12.68%, respectively of the total pore volume indicating that the PAC was of mesoporous in nature (Table 1).

3.1.7. Thermal stability of PAC

The thermogravimetric analysis of the PAC in nitrogen atmosphere exhibited three-step weight loss. The first weight loss in the range of $30\text{--}110^\circ\text{C}$ (approximately 18%) indicated the weight loss due to moisture loss from the PAC. The PAC was found to be thermally stable in the range of $150\text{--}450^\circ\text{C}$. A major weight loss was observed around $450\text{--}750^\circ\text{C}$ resulting 75% weight loss due to the decomposition of stable surface oxygen groups such as carboxyl, ethers, and hydroxyls present in the structure of the activated carbon.

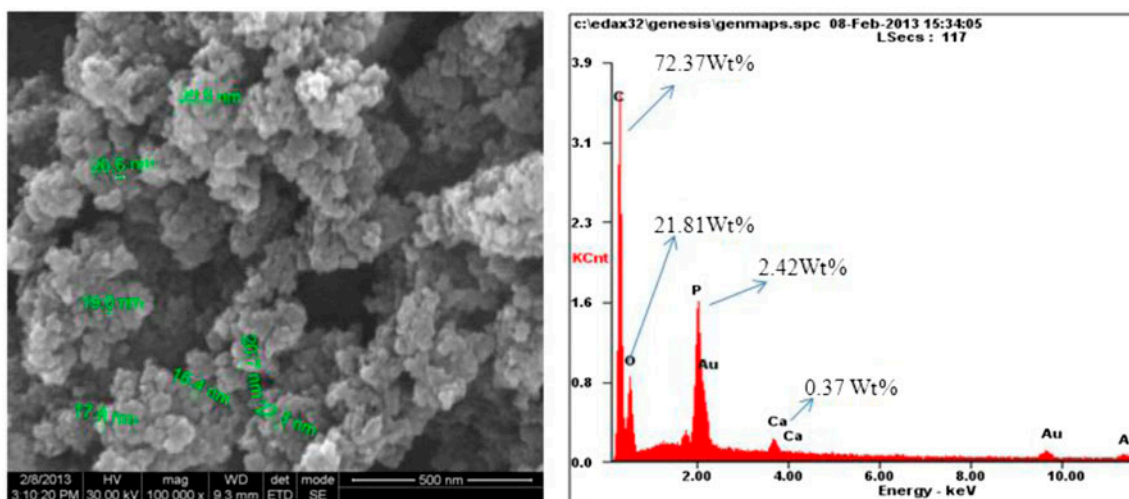


Fig. 3. (a) HR-SEM image of PAC and (b) EDAX profile of PAC.

Table 1
Physical properties of PAC

S_{BET} (m^2/g)	S_{ext} (m^2/g)	$S_{\text{ext}}/S_{\text{BET}}$ (%)	S_{mic} (m^2/g)	$S_{\text{mic}}/S_{\text{BET}}$ (%)	V_{tot} (cm^3/g)	V_{mic} (cm^3/g)	V_{mes} (cm^3/g)	$V_{\text{mic}}/V_{\text{tot}}$ (%)	$V_{\text{mes}}/V_{\text{tot}}$ (%)	D_{av} (nm)
409.01	299.05	73.11	109.96	26.88	0.439	0.055	0.381	12.68	87.32	4.3

3.1.8. Zero point charge of PAC

The pH_{zpc} of PAC was determined by salt addition method which is also called as drift method. In this method, 0.1 M KCl solution was maintained at different pH (1–12) and to this 0.1 g of PAC was added and then the suspensions were agitated for 24 h under incubation. After 24 h, the pH of the solution was determined. pH_{zpc} of activated carbon sample is the point when $\text{pH}_{\text{initial}} = \text{pH}_{\text{final}}$. At $\text{pH} < \text{pH}_{\text{zpc}}$, the surface has a net positive charge and at $\text{pH} > \text{pH}_{\text{zpc}}$, it is negative. The low pH_{zpc} value was consistent with the Boehm titration result, which showed that the acidic groups were dominant at the surface of the activated carbon. Similar type of result was observed for the activated carbon prepared from jackfruit peel [30].

3.2. Effect of contact time

The effect of contact time (Fig. 4) on the adsorption of SO was studied for different concentrations. The adsorption experiments were carried out under the regular interval of time with a fixed adsorbent dose of 0.06 g varying the concentrations of SO dye as 4×10^{-4} M, 5×10^{-4} M, and 6×10^{-4} M. The removal of

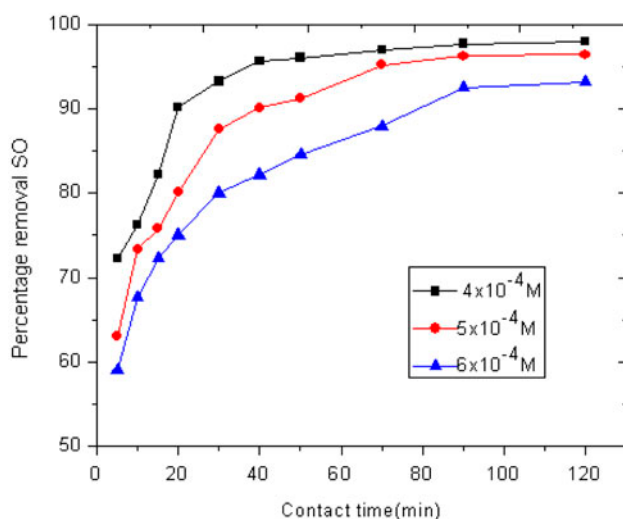


Fig. 4. Effect of contact time on the adsorption of SO by PAC (0.06 g/50 ml) SO concentration 4×10^{-4} , 5×10^{-4} , 6×10^{-4} M and at temperature 305 ± 1 K.

dye was faster in the initial stages. The dye removal slowed down in later stages and finally reached a steady state at 90 min. The optimum contact time was taken to be 120 min to study the other parameters.

3.3. Effect of adsorbent dose

Adsorbent dosage determines the adsorption capacity of an adsorbent for a given initial concentration of the adsorbate at a particular temperature. The effect of adsorbent dosage was studied for an initial dye concentration of 6×10^{-4} M/50 ml, by varying the dosage of PAC from 0.01 to 0.1 g, keeping all other parameters constant. The dye removal (Fig. 5) efficiency increased from 24.28 to 99.23% with an increase in adsorbent dosage. This might be due to the presence of more surface area and the presence of number of adsorption sites [31].

3.4. Effect of concentration at different temperatures

The removal of SO dye was studied at different temperatures of 305, 315, and 325 ± 1 K with a constant adsorbent dose of 0.06 g and at different concentrations

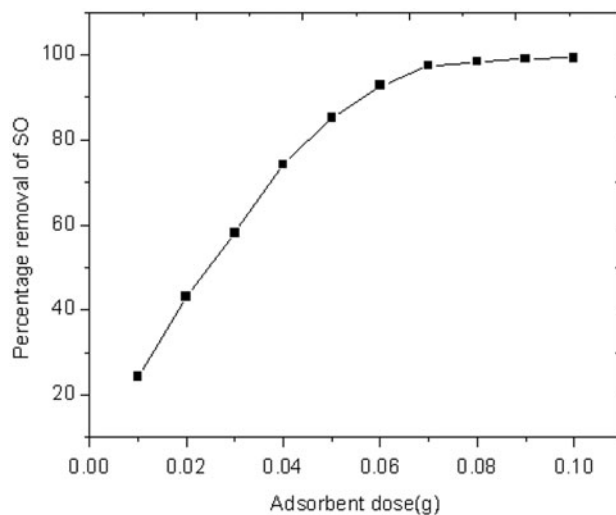


Fig. 5. Effect of PAC dose on the removal of SO (6×10^{-4} M), contact time 120 min, temperature 305 ± 1 K.

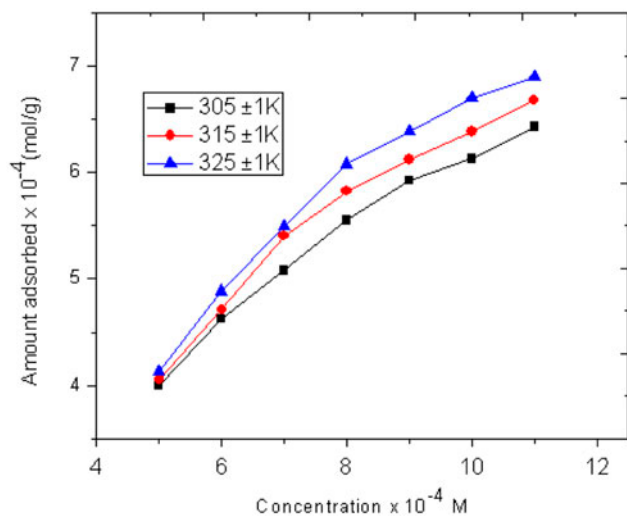


Fig. 6. Effect of concentration for the removal SO by PAC (0.06 g), contact time 120 min at different temperature.

of SO dye (5×10^{-4} to 11×10^{-4} M). The adsorption of SO dye increased with increase in temperature (Fig. 6). The positive effect of temperature on the adsorption of SO dye indicated that adsorption process is endothermic in nature. This is consistent with previous studies that the adsorption of SO onto activated carbon prepared from corn cob also increased with increase in temperature [32].

3.5. The effect of pH

The pH of a solution played an important role in the removal of SO dye from aqueous solution. The SO dye removal was investigated over (Fig. 7) a pH range of 1.0–11.5 with an adsorbent dose of 0.06 g, initial SO concentration of 6×10^{-4} M, and contact time of 120 min. The percentage removal of SO dye increased as the pH increased from 1.0 to 11.5. The pH_{zpc} of PAC was found to be 1.9. The surface of PAC is positive below pH 1.9 and above pH 1.9 the surface is negative. As the pH of the solution increased, the number of negatively charged active sites increased and positively charged sites decreased. At higher pH, the COOH groups were ionized to COO^- . Due to the electrostatic interaction between N^+ of SO dye and COO^- of PAC, the adsorption of SO dye got enhanced. The lower adsorption of SO dye in acidic medium was due to the electrostatic repulsion between the adsorbent sites (H_3O^+) and positively charged dye ion. Similar results were observed for the adsorption of SO dye over sugar beet pulp [33].

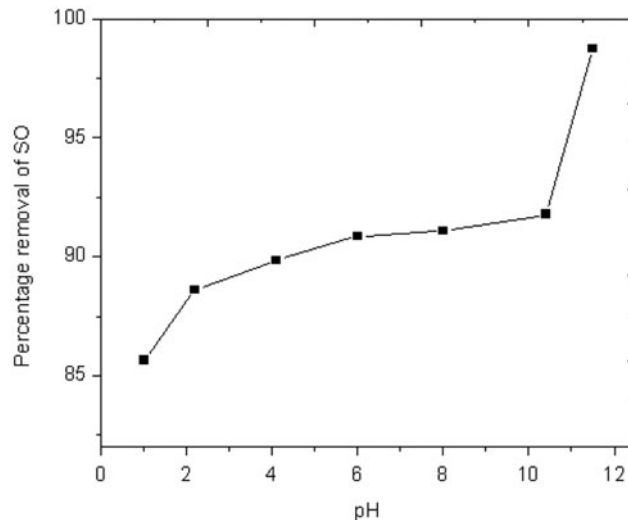


Fig. 7. Effect of pH on the adsorption of SO by PAC at contact time 120 min, PAC dose 0.06 g/50 ml, SO concentration 6×10^{-4} M, temperature 305 ± 1 K.

3.6. Adsorption isotherms

Adsorption isotherms are used to determine the adsorption capacity of the adsorbent at a particular temperature, to describe the adsorption progress and to investigate the adsorption mechanism. The variation of the adsorbate concentration with the known weight of the adsorbent is applied to describe the adsorption mechanism at constant temperature [34]. Langmuir, Freundlich, and Dubinin–Radushkevich adsorption isotherms were applied for the adsorption of SO dye over the surface of PAC (Table 1).

3.6.1. Langmuir adsorption isotherm

The Langmuir adsorption isotherm is valid for monolayer coverage of the adsorbate onto surface of adsorbent with a finite number of adsorption sites [34]. This is specifically used to determine the maximum adsorption capacity of the adsorbent [35].

The plots of C_e vs. C_e/q_e gave straight lines with regression coefficients close to unity confirming the applicability of Langmuir isotherm model in the present study. The values of the adsorption capacity (Q_m), and the Langmuir equilibrium constant (K_L), were calculated from the slope and intercept of the linear plots of C_e vs. C_e/q_e and are shown in Table 2.

The feasibility of Langmuir adsorption isotherm was tested using dimensionless constant called separation factor or equilibrium parameter (R_L) which is defined by the following equation [36]:

Table 2
Adsorption isotherm parameters for adsorption of SO onto PAC

Adsorption isotherm	Temperature		
	305 ± 1 K	315 ± 1 K	325 ± 1 K
<i>Langmuir isotherm</i>			
Q_m (mol/g)	6.325×10^{-4}	6.522×10^{-4}	6.765×10^{-4}
K_L (L/mol)	7.343×10^4	10.967×10^4	18.756×10^4
R^2	0.995	0.997	0.997
R_L	0.026	0.018	0.01
<i>Freundlich isotherm</i>			
K_f (mol/g)	2.184×10^{-3}	2.221×10^{-3}	2.410×10^{-3}
n	6.439	6.709	6.829
R^2	0.992	0.988	0.982
<i>Dubinin–Radushkevich isotherm</i>			
Q_m (mol/g)	1.013×10^{-3}	1.033×10^{-3}	1.188×10^{-3}
K (mol ² /KJ ²)	0.1192×10^{-8}	0.1026×10^{-8}	0.1023×10^{-8}
E (kJ/mol)	20.480	22.075	22.107
R^2	0.979	0.972	0.974

$$R_L = \frac{1}{K_L C_0} \quad (2)$$

where C_0 is the initial SO dye concentration (mol/L) and K_L (L/mol) is Langmuir equilibrium constant. If R_L is greater than 1, the type of adsorption isotherm is unfavorable and if R_L is 0–1, that adsorption isotherm is favorable. The R_L value in the range of 0–1 also confirmed the favorable adsorptive uptake of dye process. The applicability of the Langmuir isotherm suggests the monolayer coverage of the SO dye molecules onto PAC and homogeneous distribution of active sites of PAC surface.

The monolayer adsorption capacity of SO dye—PAC system was found to be 6.325×10^{-4} mol/g (221.91 mg/g) which is much higher than that of other low-cost adsorbents [33,37–39]. Therefore the obtained PAC can be used in the wastewater treatment and has the potential to be replaced with the expensive adsorbents available in the market.

3.6.2. Freundlich adsorption isotherm

The Freundlich adsorption isotherm assumes [40] that the adsorption takes place on heterogeneous surface as well as multilayer sorption.

The plots of $\log(q_e)$ vs. $\log(C_e)$ indicated the applicability of Freundlich isotherm. The values of n are the range of 1–10, indicates that the adsorption is favorable [41]. The Freundlich constants K_L and n values were presented in Table 2. The n values are found to be between 6.4 and 6.8 for SO dye and hence the adsorption of SO dye over PAC is favorable. The

values of Q_m and K_f increased (Table 2) with increase in temperature indicating that the adsorption process was endothermic in nature.

3.6.3. Dubinin–Radushkevich adsorption isotherm

Dubinin–Radushkevich adsorption isotherm is used to describe the adsorption on both homogeneous and heterogeneous surfaces. It is applied to find out whether the adsorption is taking place by physical or chemical processes. The linear form of the isotherm can be expressed as follows [42].

$$\ln(q_e) = \ln(Q_m) - K\varepsilon^2 \quad (3)$$

where K (mol²/KJ²) is constant related to the adsorption constant, and ε is the Polanyi potential that can be calculated from the following equation:

$$\varepsilon = RT \ln\left(1 + \frac{1}{C_e}\right) \quad (4)$$

where T is the temperature in Kelvin (K) and R is the Universal gas constant (8.314 J/mol/K).

The constant K , (slope of $\ln(q_e)$ vs. ε^2) gives the mean free energy of sorption, E (kJ/mol) and is calculated using the following equation:

$$E = \frac{1}{\sqrt{(2K)}} \quad (5)$$

Dubinin–Radushkevich adsorption isotherm was employed for the adsorption equilibrium experimental data. The value E is useful for determining the adsorption mechanism. If the value of E is less than 8 kJ/mol, then the adsorption takes place by physical forces. If E is in the range of 8–16 kJ/mol, adsorption occurs by ion-exchange mechanism. When E is greater than 16 kJ/mol, it indicates that the adsorption process is of chemisorption in nature [43]. From the experimental study, the value of E was found to be greater than 16 kJ/mol (20.480–22.107 kJ/mol), which showed that the adsorption of SO dye over the surface of PAC followed the chemisorption process.

Comparing the R^2 (Table 2) values of the three adsorption isotherm models, the Langmuir model provided the highest R^2 of 0.999 which implies that it is the best fit in describing the adsorption of SO dye onto PAC.

3.7. Adsorption kinetics

Pseudo-first-order and pseudo-second-order kinetic equations were used to fit the experimental data to evaluate the mechanism of adsorption process.

3.7.1. Pseudo-first-order equation

The adsorption kinetic data were described by the Lagergren pseudo-first-order model [44,45] which describes the adsorption rate based on the adsorption capacity. The pseudo-first-order equation is expressed as follows:

$$\log(q_e - q_t) = \log q_e - \frac{k_1 t}{2.303} \quad (6)$$

Thus the rate constant k_1 (1/min) and q_e can be calculated from the slope and intercepts of $\log(q_e - q_t)$ vs. time t . If the calculated q_e value is equal to the experimental q_e , then it could suggest that the adsorption follows the pseudo-first-order kinetics [46,47].

The plots of $\log(q_e - q_t)$ vs. t give a straight line with high correlation coefficients ranging from 0.954 to 0.980. The first-order-kinetic parameters k_1 , R^2 , and q_e are reported in Table 3. The values of $q_e(\text{calc})$ were found to increase with increasing concentration of the SO dye. Even though the correlation coefficients are high, the $q_e(\text{calc})$ values are not equal to the $q_e(\text{exp})$. Therefore the adsorption of SO dye onto PAC does not follow the pseudo-first-order kinetics.

3.7.2. Pseudo-second-order kinetics

The pseudo-second-order kinetic rate equation is expressed as follows [45,48]:

$$\frac{t}{q_t} = \frac{1}{k_2 q_e^2} + \frac{1}{q_e} t \quad (7)$$

The plots of t/q_t vs. t were straight lines for all the initial concentrations studied, suggesting that the adsorption process followed the pseudo-second-order kinetic model at the entire adsorption contact time of 120 min. The second-order kinetic parameters k_2 , $q_e(\text{calc})$, and R^2 are listed in Table 3. The correlation coefficients were nearly equal to unity and the $q_e(\text{calc})$ values were in good agreement with the $q_e(\text{exp})$ data, which confirmed that the adsorption of SO dye onto PAC surface followed pseudo-second-order kinetics.

3.8. Adsorption thermodynamics

Thermodynamic parameters such as ΔG° , ΔH° , and ΔS° were determined to evaluate the spontaneity and the nature of the adsorption process [47]. These values were calculated using the following relationships:

$$\Delta G^\circ = -RT \ln K_L \quad (8)$$

ΔH° and ΔS° values were estimated from the following equations.

Table 3

Pseudo-first-order and pseudo-second-order kinetic parameters for the adsorption of SO onto PAC

Adsorbate conc (M)	$q_e(\text{exp})$ (mol/g)	Pseudo-first-order			Pseudo-second-order		
		k_1 (1/min)	$q_e(\text{calc})$ (mol/g)	R^2	k_2 (g/mol min)	$q_e(\text{calc})$ (mol/g)	R^2
4.0×10^{-4}	2.998×10^{-4}	0.048	0.940×10^{-4}	0.964	11.67×10^4	3.355×10^{-4}	0.999
5.0×10^{-4}	3.544×10^{-4}	0.049	1.902×10^{-4}	0.980	5.40×10^4	4.208×10^{-4}	0.999
6.0×10^{-4}	3.971×10^{-4}	0.039	2.170×10^{-4}	0.954	3.90×10^4	4.821×10^{-4}	0.999

$$\Delta H^\circ = -R \frac{T_2 T_1}{T_2 - T_1} \ln \frac{K_{L1}}{K_{L2}} \quad (9)$$

where K_L , K_{L1} , and K_{L2} are the Langmuir constants at different temperatures, R is the universal gas constant (8.314 J/mol/K), and T is the Kelvin temperature.

$$\Delta S^\circ = \frac{\Delta H^\circ - \Delta G^\circ}{T} \quad (10)$$

The negative values of ΔG° (–28.41, –30.393, and –32.80 kJ/mol) in the temperature range of 305–325 K, showed that the process was of spontaneous in nature. ΔH° and ΔS° were calculated as 45.67 kJ/mol and 242.90 J/mol/K for SO dye, respectively. The positive values of ΔH° and ΔS° indicated that the adsorption process was of endothermic in nature and the adsorption mechanism was an entropy controlled process.

4. Conclusions

Removal of SO dye from aqueous solution by adsorption with activated carbon prepared from *P. pterocarpum* leaf powder has been experimentally determined and the following observations are made:

- (1) The PAC is graphitic, nanocrystalline, and the surface is mesoporous.
- (2) The monolayer adsorption capacity of SO dye–PAC system was found to be 6.325×10^{-4} mol/g (221.91 mg/g).
- (3) The mean free energy of sorption (E) value was found to be 20.48 kJ/mol, indicating that chemisorption might be the major mode in the adsorption of SO.
- (4) The adsorption kinetics of SO dye with PAC followed the pseudo-second-order kinetics because the calculated q_e values and experimental values of q_e were in good agreement.
- (5) The negative values of ΔG° and the positive value of ΔH° indicated the process was spontaneous and endothermic in nature. It was due to high positive value of ΔS° that the adsorption became spontaneous.

The PAC effectively removes SO from aqueous solution and its adsorption capacity is much higher than that of other low cost adsorbents. Hence the PAC can be efficiently used for the adsorptive removal of dyes from real effluents from the dye industries in near future.

References

- [1] T. Robinson, G. McMullan, R. Marchant, P. Nigam, Remediation of dyes in textiles effluent: A critical review on current treatment technologies with a proposed alternative, *Bioresour. Technol.* 77 (2001) 247–255.
- [2] S.K. Theydan, M.J. Ahmed, Adsorption of Methylene Blue onto biomass based activated carbon by FeCl₃ activation: Equilibrium, kinetics and thermodynamic studies, *J. Anal. Appl. Pyrol.* 97 (2012) 116–122.
- [3] R.J. Stephenson, J.B. Sheldon, Coagulation and precipitation of a mechanical pulping effluent—I. Removal of carbon, colour and turbidity, *Water Res.* 30 (1996) 781–792.
- [4] E. Forgacs, C. Tibor, O. Gyula, Removal of synthetic dyes from wastewaters: A review, *Environ. Int.* 30 (2004) 953–971.
- [5] H. Wu, Y. Xie, J. Zhao, H. Hidaka, Photo-Fenton degradation of a dye under visible light irradiation, *J. Mol. Catal. A: Chem.* 144 (1999) 77–84.
- [6] E. Kusvuran, O. Gulnaz, S. Irmak, O.M. Atanur, H. Yavuz, O. Erbatur, Comparison of several advanced oxidation processes for the decolorization of Reactive Red 120 azo dye in aqueous solution, *J. Hazard. Mater.* 109 (2004) 85–93.
- [7] H. Daraei, A. Mittal, M. Noorisepehr, J. Mittal, Separation of chromium from water samples using eggshell powder as low cost sorbent: Kinetic and thermodynamic studies, doi: [10.1080/19443994.2013.837011](https://doi.org/10.1080/19443994.2013.837011).
- [8] H. Daraei, A. Mittal, M. Noorisepehr, F. Daraei, Kinetic and equilibrium studies of adsorptive removal of phenol onto eggshell waste, *Environ. Sci. Pollut. Res.* 20 (2013) 4603–4611.
- [9] C.K. Lee, S.S. Liu, L.C. Juang, C.C. Wang, K.S. Lin, M. Du Lyu, Application of MCM-41 for dyes removal from wastewater, *J. Hazard. Mater.* 147 (2007) 997–1005.
- [10] S.J. Allen, B. Koumanova, Decolourisation of water/wastewater using adsorption (review), *J. Univ. Chem. Technol. Metall.* 40 (2005) 175–192.
- [11] J. Mittal, D. Jhare, H. Vardhan, A. Mittal, Utilization of bottom ash as low cost sorbent for the removal and recovery of a toxic halogen containing dye eosin yellow, doi: [10.1080/19443994.2013.803265](https://doi.org/10.1080/19443994.2013.803265).
- [12] A. Mittal, L. Kurup, Column operation for the removal and recovery of a hazardous dye acid red 27 from aqueous solutions, using waste materials bottom ash and de oiled soya, *Ecol. Environ. Conserv.* 12 (2006) 181–186.
- [13] A. Mittal, Adsorption kinetics of removal of a toxic dye, malachite green, from wastewater by using hen feathers, *J. Hazard. Mater.* 133 (2006) 196–202.
- [14] A. Mittal, V. Thakur, J. Mittal, H. Vardhan, Process development for the removal of hazardous anionic azo dye Congo red from wastewater by using hen feather as potential adsorbent, *Desalin. Water Treat.* 52 (2014) 227–237.
- [15] A. Mittal, Removal of the dye Amarnath from wastewater using hen feather as potential adsorbent, *Elec. J. Environ. Agric. Food Chem.* 5 (2006) 1296–1305.
- [16] J. Mittal, V. Thakur, A. Mittal, Batch removal of hazardous azo dye Bismark brown R using waste material hen feather, *Ecol. Eng.* 60 (2013) 249–253.

- [17] A. Mittal, Use of hen feathers as potential adsorbent for the removal of a hazardous dye, brilliant blue FCF, from wastewater, *J. Hazard. Mater.* 128 (2006) 233–239.
- [18] A. Mittal, J. Mittal, L. Karup, Utilization of hen feathers for the adsorption of Indigo carmine from simulated effluents, *J. Environ. Prot. Sci.* 1 (2007) 92–100.
- [19] R.R. Bansode, J.N. Losso, W.E. Marshall, R.M. Rao, R.G. Portier, Adsorption of metal ions by pecan shell-based granular activated carbons, *Bioresour. Technol.* 89 (2003) 115–119.
- [20] H.M.H. Gad, A.A. El-Sayed, Activated carbon from agricultural by-products for the removal of Rhodamine-B from aqueous solution, *J. Hazard. Mater.* 168 (2009) 1070–1081.
- [21] K. Hayat, M.A. Gondal, M.M. Khaled, Z.H. Yamani, S. Ahmed, Laser induced photocatalytic degradation of hazardous dye (Safranin-O) using self-synthesized nanocrystalline WO_3 , *J. Hazard. Mater.* 186 (2011) 1226–1233.
- [22] M. Shafiq, M. Zafar Iqbal, Germination and seedling behaviours of seeds of *Peltophorum Pterocarpum* D.C. Baker Ex K. Heyne Growing under motor vehicle emission, *Turk. J. Bot.* 31 (2007) 565–570.
- [23] Q.S. Liu, T. Zheng, P. Wang, L. Guo, Preparation and characterization of activated carbon from bamboo by microwave induced phosphoric acid activation, *Ind. Crops Prod.* 31 (2010) 233–238.
- [24] B. Viswanathan, P. Indra Neel, T.K. Varadarajan, Development of carbon materials for energy and environmental applications. *Catal. Surv. Asia.* 13 (2009) 164–183.
- [25] M. Benadjemi, L. Milliere, L. Reinert, N. Benderdouche, L. Duclaux, Preparation, characterization and methylene blue adsorption of phosphoric acid activated carbons from globe artichoke leaves, *Fuel Process. Technol.* 92 (2011) 1203–1212.
- [26] H. Liu, X. Wang, G. Zhai, J. Zhang, C. Zhang, N. Bao, C. Cheng, Preparation of activated carbon from lotus stalks with the mixture of phosphoric acid and pentaerythritol impregnation and its application for Ni(II) sorption, *Chem. Eng. J.* 209 (2012) 155–162.
- [27] M.D.G. de Laun, E.D. Flores, D.A.D. Genuino, C.M. Futralan, M.W. Wan, Adsorption of Eriochrome Black T (EBT) dye using activated carbon prepared from waste rice hulls – Optimization, isotherm and kinetic studies, *J. Taiwan Inst. Chem. Eng.* 44 (2013) 646–653.
- [28] J.S. Nazzal, W. Kaminska, B. Michalkiewicz, Z.C. Koren, Production, characterization and methane storage potential of KOH-activated carbon from sugarcane molasses, *Ind. Crops Prod.* 47 (2013) 153–159.
- [29] X. Yuan, D. Yuan, F. Zeng, W. Zou, F. Tzorbatzoglou, P. Tsiakaras, Y. Wang, Preparation of graphitic mesoporous carbon for the simultaneous detection of hydroquinone and catechol, *Appl. Catal. B: Environ.* 129 (2013) 367–374.
- [30] D. Prahast, Y. Kartika, N. Indraswati, S. Ismadji, Activated carbon from jackfruit peel waste by H_3PO_4 chemical activation: Pore structure and surface chemistry characterization, *Chem. Eng. J.* 140 (2008) 32–42.
- [31] C. Namasivayam, D. Kavitha, Removal of Congo red from water by adsorption onto activated carbon prepared from coir pith, an agriculture solid waste, *Dyes Pigm.* 54 (2000) 47–58.
- [32] S. Preethi, A. Sivasamy, S. Sivanesan, V. Ramamurthi, G. Swaminathan, Removal of Safranin basic dye from aqueous solutions by adsorption onto corncob activated carbon, *Ind. Eng. Chem. Res.* 45 (2006) 7627–7632.
- [33] M. RasoolMalekbala, S. Hosseini, S. KazemiYazdi, S. Masoudi Soltani, M. Rahim Malekbala, The study of the potential capability of sugar beet pulp on the removal efficiency of two cationic dyes, *Chem. Eng. Res. Des.* 90 (2012) 704–712.
- [34] Ö Gök, A. Özcan, A. Özcan, Adsorption behavior of a textile dye of reactive blue 19 from aqueous solutions onto modified bentonite, *Appl. Surf. Sci.* 256 (2010) 5439–5443.
- [35] S. Eftekhari, A. Habibi-Yangjeh, SH Sohrabnezhad, Application of AlMCM-41 for competitive adsorption of methylene blue and rhodamine B: Thermodynamic and kinetic studies, *J. Hazard. Mater.* 178 (2010) 349–355.
- [36] I.D. Mall, V.C. Srivastava, G.V.A. Kumar, I.M. Mishra, Characterization and utilization of mesoporous fertilizer plant waste carbon for adsorptive removal of dyes from aqueous solution, *Colloids Surf. A: Physicochem. Eng. Aspects* 278 (2006) 175–187.
- [37] S. Gokturk, S. Kaluc, Removal of selected organic compounds in aqueous solutions by activated carbon, *J. Environ. Sci. Technol.* 3 (2008) 111–123.
- [38] S. Chowdhury, R. Mishra, P. Kushwaha, P. Saha, Removal of Safranin from aqueous solutions by NaOH-treated rice husk: Thermodynamics, kinetics and isosteric heat of adsorption, *Asia-Pac. J. Chem. Eng.* 7 (2012) 236–249.
- [39] I. Safarik, M. Safarikova, Magnetic fluid modified peanut husks as an adsorbent for organic dyes removal, *Phys. Procedia* 9 (2010) 274–278.
- [40] G. Crini, H.N. Peindy, F. Gimbert, C. Robert, Removal of C.I. basic green 4 (malachite green) from aqueous solutions by adsorption using cyclodextrin-based adsorbent: Kinetic and equilibrium studies, *Sep. Purif. Technol.* 53 (2007) 97–110.
- [41] Y. Bulut, H. Aydın, A kinetics and thermodynamics study of methylene blue adsorption on wheat shells, *Desalination* 194 (2006) 259–267.
- [42] C. Namasivayam, N. Kanchana, Waste banana pith as adsorbent for color removal from wastewaters, *Chemosphere* 25 (1992) 1691–1706.
- [43] K.V. Kumar, V. Ramamurthi, S. Sivanesan, Modeling the mechanism involved during the sorption of methylene blue onto fly ash, *J. Colloid Interface Sci.* 284 (2005) 14–21.
- [44] H. Zhang, Y. Tang, X. Liu, Z. Ke, Xi. Su, D. Cai, X. Wang, Y. Liu, Q. Huang, Z. Yu, Improved adsorption capacity of pine wood decayed by fungi *Poria cocos* for removal of malachite green from aqueous solutions, *Desalination* 274 (2011) 97–104.
- [45] J. Zhang, Y. Li, C. Zhang, Y. Jing, Adsorption of malachite green from aqueous solution onto carbon prepared from arundo donax root, *J. Hazard. Mater.* 150 (2008) 774–782.
- [46] E. Bulut, M. Ozacar, I.A. Sengil, Adsorption of malachite green onto bentonite: Equilibrium and kinetic studies and process design, *Microporous Mesoporous Mater.* 115 (2008) 234–246.

- [47] S. Wang, Z.H. Zhu, Characterization and environmental application of an Australian natural zeolite for basic dye removal from the aqueous solution, *J. Hazard. Mater.* 136 (2006) 946–952.
- [48] Y.S. Ho, G. Mckay, A comparison of chemisorption kinetic models applied to pollutant removal on various sorbents, *Process Saf. Environ. Prot.* 76 (1998) 332–340.